EVALUATION AND PREDICTION OF SHEAR WAVE VELOCITIES IN SOFT MARINE SEDIMENTS

by

J.A. Meredith

Earth Resources Laboratory
Department of Earth, Atmospheric, and Planetary Sciences
Massachusetts Institute of Technology
Cambridge, MA 02139

R.H. Wilkens

Hawaii Institute of Geophysics
University of Hawaii, Manoa Campus
Honolulu, Hawaii 96822

C.H. Cheng

Earth Resources Laboratory
Department of Earth, Atmospheric, and Planetary Sciences
Massachusetts Institute of Technology
Cambridge, MA 02139

ABSTRACT

Shear wave velocities from full waveform acoustic logs were determined at DSDP Site 613 using the spectral ratio inversion method. Discrete shear wave velocities for a 350 meter interval at 0.5–2 meter depth increments were calculated. Shear wave velocities were not evaluated for the upper 130m of the log because of data recording problems. The sediments of Site 613 represent a progression from carbonaceous-siliceous oozes through partial lithification and cementation. A method for predicting shear wave velocities using Wood's equation, the bulk moduli of water and carbonate grains, the P-wave velocity and porosity from well logs will be described. The predictions of this method provided a theoretical maximum value for the shear wave velocity to compare with the inversion results. In general, the method works well for shear wave velocities greater than 800 m/s. The inverted data fall just below the predicted theoretical maximum value from Wood's equation and agree quite well with the trends. Below this velocity threshold, trends with depth and Poisson's ratio and the divergence of

the inversion itself seem to indicate incorrect behavior.

INTRODUCTION

The shear wave velocity of marine sediments is of interest to a large number of marine studies. In particular, the shear wave velocity (and thus the shear wave modulus) is of importance in the study of the state of compaction and cementation of marine sediments. However, shear wave velocity measurements from cores are very difficult and seldom done, mainly because of the difficulty in the preservation of core samples from these unconsolidated and semi-consolidated sediments. Until recently, in situ measurements from full waveform acoustic logs in these sediments have not been possible because of the lack of refracted shear waves in these low velocity sediments and the lack of excitation of Stoneley waves at the frequency of existing logging tools. Cheng (1987) was the first to utilize the refracted P wave and its associated leaky modes to invert for the shear wave velocity of the formation under these conditions. In this paper, we apply this technique to obtain estimates of shear wave velocity in marine sediments and compare them to the upper bound obtained using Wood's (1941) equation and the P-wave velocity from the full waveform log, as well as lithology, density, and porosity information from both logs and core analysis.

The logging data were from the Baltimore Canyon Trough (DSDP Site 613) with a 2300 meter ocean bottom depth. Three major lithological units were logged. Unit 1, the uppermost layer, Eocene in age, represented clay rich terrigenous deposition. Units 2 and 3 were comprised of siliceous carbonate oozes with very little clay content (Wilkens et al., 1985). The major difference between Units 2 and 3 is a phase change in the silica component from opal to porcellanite resulting in a 15-20% decrease in porosity and an increase in bulk modulus. This boundary between Units 2 and 3 is a widely recognized reflector in seismic data taken in the area.

Logging began at 120 meters below sea floor (mbsf) depth in Unit 1 and proceeded into Unit 2 from 279 mbsf to 442 mbsf and finished at a bottom hole depth of 570 meters in Unit 3. Unfortunately, the full waveform acoustic logs from Unit 1 were normalized without maintaining relative amplitudes so could not be processed. However, we did obtain shear wave velocities for Unit 2 and Unit 3. Results from Unit 3 correlate well with predicted maximum shear wave velocities. The convergence properties for the Unit 3 results were excellent but were not good for the Unit 2 results. This would indicate that there are upper bounds on Poisson's ratio above which the technique does not work very well.

INVERSION TECHNIQUE

The inversion technique has been presented previously in Cheng (1987), and the use of the technique in Meredith et al. (1987). We will briefly review the basic details here.

It is assumed that the source function from the logging tool inside the borehole is unknown so a method not dependent on source properties is required. A data set taken over a multi-source, multi-receiver array will contain many pairs of time series data taken over the same positions. The Fourier spectra of data from a given receiver pair are obtained using the Fast Fourier Transform (FFT). By the convolution model, the FFT is modelled in the frequency domain by a transfer function multiplied by a source function. Assuming that the source function, although unknown, is independent of depth, and the receivers are equalized, the quotient of the two inversions yields a ratio of transfer functions. The source functions cancel each other as shown below:

$$\frac{FFT\ 1\ \rightarrow\ S(\omega) \bullet H_1(\omega)}{FFT\ 2\ \rightarrow\ S(\omega) \bullet H_2(\omega)} \ . \tag{1}$$

This data transfer function ratio is approximated by a ratio of the computed Green's functions. In order to isolate the P wave contribution to the Green's function from the S and guided waves, we use the branch-cut integral method of Tsang and Rader (1979). V_s and Q_p are parameters in the branch cut integral and by assuming all other parameters are known, an object function for V_s and Q_p can be established. A standard damped least squares inversion procedure is applied to the object function to obtain estimates of V_s and Q_p.

As in any inversion problem, the accuracy of the inversion depends on two factors: 1) the closeness of the forward model used to the actual situation in which the data is collected; and 2) numerical accuracy involved in the calculation of the forward model and its Jacobian partial derivative matrix. We have approximated the forward model by ignoring the tool and reducing the radius of the borehole to compensate for it. This is reasonable for a steel body tool such as that used in the collection of our data, especially for the first normal or leaky mode (Cheng and Toksöz, 1981). This assumption gets progressively worse for the higher modes, and could be a contributor to the breakdown of the method at low shear wave velocities. The numerical accuracy of the branch integral is in general very good (Kurkjian, 1985) for the higher velocity materials and less so for very low velocity materials, because a larger number of terms needs to be included and numerical errors can accumulate. We will further discuss these issues and how they affect our results in a later section.

PREDICTION OF SHEAR WAVE VELOCITIES

The Acoustic Index

The compressional wave velocity of unconsolidated marine sediments is dictated almost entirely by the porosity of those sediments (Wood, 1941; Hamilton, 1971). Intrinsic differences in individual sediment grain elastic moduli have little effect on the velocity of a mixture dominated by the properties of water. Thus, uncemented sediments of the same porosity will have virtually the same compressional wave velocity regardless of mineralogy. The compressional wave velocity of sedimentary rocks, on the other hand, is controlled not only by porosity, but also by the mineralogy of the grains and the extent to which those grains are cemented into a solid framework (Ogushwitz, 1985; Wilkens et al., 1986). Much the same can be said of the shear wave velocity of sediments and sedimentary rocks. Mixtures of loose grains have little rigidity and low shear wave velocities, regardless of the elastic moduli of the grains themselves. Cementation at grain to grain contacts increases the shear modulus of the aggregate. Eventually the moduli of the sediment particles will influence the rigidity of the framework of the welded grains.

Samples recovered from near the seafloor behave according to systematics of a seawater dominated system. Samples from progressively deeper in the sedimentary column behave more like sedimentary rocks as they lose porosity and become increasingly cemented. Numerous theoretical developments have addressed the properties of either loose sediment grains or sedimentary rocks, but there has been little work on the domain of sediments which are undergoing lithification, and behave unlike either loose sediments or rocks. We require a system that will yield some quantification of the porosity-velocity relationship of these materials so that we can better describe the continuum of change from one state to the other. In particular, a method which will remove the first order effects of porosity on velocity and emphasize the effects of cementation will add to our understanding of sediment shear wave velocities.

We have chosen the Wood and Wyllie equations (Wood, 1941; Wyllie et al., 1956) to represent end points of the progression from ooze to sedimentary rock. These are simple formulations that represent well understood concepts. Neither equation is exactly correct (Wyllie's equation is in fact empirical), but both describe general velocity-porosity relationships.

Wood's equation (Wood, 1941) is used to describe the acoustic velocity of a mixture of loose grains and fluid. The theory assumes that the shear modulus of a high porosity aggregate of fluid and grains is zero and that its bulk modulus is equal to a geometric average of the bulk moduli of the grains and fluid. The effective bulk modulus of the medium is computed by:

$$K_{sed} = \frac{\Phi}{K_w} + \frac{1-\Phi}{K_g}$$

where K_w is the bulk modulus of seawater, Φ is porosity expressed as a fraction, and K_g is the grain bulk modulus. Bulk densities are computed using the densities of seawater and grains. The compressional wave velocity is computed by:

$$V_p = \sqrt{\frac{K_{sed} + 4\mu/3}{\rho}}$$

where ρ is the bulk density of the seawater-sediment mixture and μ is the mixture shear modulus, assumed here to be zero. While Wood's equation has been shown to work well in describing the behavior of controlled laboratory clay mixtures of high porosity material (Ogushwitz, 1985), Hamilton (1982) has demonstrated that the zero shear modulus assumption is invalid for marine sediment. Hamilton's work and the discussion below illustrate the lack of fit of Wood's equation, and also how it can be used to estimate shear wave velocities.

The Wyllie time-average equation (Wyllie et al., 1956) is an empirical formulation used to represent velocity-porosity relationships for sedimentary rocks. It has the same form as the Wood equation but uses grain and fluid velocities rather than bulk moduli:

$$V_p = \frac{\Phi}{V_{pw}} + \frac{1-\Phi}{V_{pg}}$$

where the subscripts are as above. The time-average equation works reasonably well for sandstones and limestones in the porosity range of about 0 to 30%. The value of velocity obtained from the Wyllie equation for high porosity carbonate sediments is not meaningful in real terms, because sedimentary rocks generally have porosities considerably lower than uncemented sediments.

The term, "Acoustic Index" or simply "Index" (Wilkens et al., 1989) will be used in this study to characterize the amount to which the velocity-porosity behavior of the sediments departs from the behavior of uncemented grains (Wood's equation) and approaches that of sedimentary rock (Wyllie's equation). The Index is defined as:

$$Acoustic\ Index = \frac{V_{p_{meas}} - V_{p_{Wood}}}{V_{p_{Wyllie}} - V_{p_{Wood}}}$$

where $V_{p_{meas}}$ is the measured velocity, $V_{p_{Wood}}$ is the computed velocity of uncemented grains with the same porosity as the sample, and $V_{p_{Wyllie}}$ is the computed velocity of a fully cemented limestone. Thus a sample whose measured velocity is equal to that

predicted by Wood's equation will have an Index of 0.0 while a sample with a measured velocity halfway between Wood's and Wyllie's predictions will have an Index of 0.5.

Following the discussion of Hamilton (1971), it is possible to use the Wood's equation to obtain an estimate of the maximum value of the shear wave velocity of loose sediments from compressional wave velocity and porosity data alone. If we assume that the calculated value of the bulk modulus of uncemented sediments is close to the true bulk modulus, then the difference between a compressional wave velocity predicted by Wood's equation (Wood's V_p) and the measured compressional wave velocity is essentially due to the error in Wood's assumption of a zero shear modulus. Inserting in the equation for compressional wave velocity the measured velocity and density and the Wood's bulk modulus we can solve for the shear modulus as follows:

$$\frac{3}{4}(V_{pmeas}^2 \rho - K_{sed}) = \mu \, . \tag{2}$$

In effect, we are attributing all of the difference between Wood's V_p and true velocity to some non-zero value of the shear modulus (Wood's shear modulus). A shear wave velocity can then be calculated from Wood's shear modulus and density (Wood's V_s).

DATA ANALYSIS

The concept of a diagenetically induced change in marine sediment velocity-porosity systematics is illustrated by data from Site 613 plotted in Figure 1. Unit 2 at Site 613 is a soft chalk with small amounts of calcite cement. The Unit 2 – Unit 3 boundary is defined by the transformation of biogenic opal-A to a denser form, opal-CT. The opal-CT is an effective cement, and the Unit 3 sediments are stiffer than those of Unit 2. The data illustrate the porosity control of velocity. It is tempting to fit a linear regression line to the data, but the relative positions of the Wood and Wyllie curves suggest that something more is happening to the sediments than a simple change of velocity with porosity. In fact, as the sediments undergo diagenesis, they begin to both lose porosity and to behave less like loose grains and more like sedimentary rock. As porosity is reduced the trend of the data is away from the Wood relationship and towards the values predicted by Wyllie's equation.

Profiles of porosity, compressional wave velocity, and Acoustic Index at Site 613 are displayed in Figure 2. Porosity generally decreases with depth as velocity increases, consistent with the relationship seen in Figure 1. The Index also increases with depth and mirrors changes seen in the logging data. It is interesting to note the character of the Index immediately above and below the Unit 2 – Unit 3 boundary. Examination of the core at Site 613 showed that recrystallized silica was concentrating in layers of harder sediments interspersed with more calcareous, less cemented intervals (Wilkens

et al., 1986). The Index appears to be able to identify the more and less cemented intervals better than either porosity or velocity alone.

Inversion results and calculation of Wood's V_s are plotted versus depth in Figure 3 and as a crossplot in Figure 4. The data can be separated into two groups: generally from depths above and below 340 mbsf (meters below sea floor). The inversion results from above this horizon appear to be incorrect. In order for the true shear wave velocity to be greater than Wood's V_s, the true bulk modulus of the sediments must be less than Wood's bulk modulus estimation. Perhaps even more of a conceptual problem is that the inversion results show the shear wave velocity decreasing over the interval 275 – 340 mbsf as the compressional wave velocity increases (Figure 2). Clearly the inversion process breaks down at very low shear wave velocities.

Data from below 340 mbsf appear well correlated to Wood's V_s. Above a Wood's V_s of 0.8 km/sec most of the inversion results are less than Wood's prediction. The inversion data tend to diverge further from the theoretical calculations as the shear wave velocity increases. This divergence is due to the assumption that all of the compressional wave velocity difference between Wood's V_p and the velocity log is due to increases in the shear modulus. This assumption is probably near correct at very high porosities, but less so as porosity decreases and cementation acts to increase both shear and bulk moduli.

It is useful to examine the relationship between the dynamic moduli defined by the shear wave velocity inversion process, the moduli calculated using Wood's equation, and the Acoustic Index. Plots of the Index versus ratios of the two bulk and shear moduli are shown in Figures 5 and 6. Disregarding the data for which we feel that the inversion results are invalid, there is a strong correlation between the value of the Index and the ratio of the theoretical and actual moduli. For low values of the Index both the shear and bulk moduli are nearly equal to the Wood's prediction. As the Index increases (and the sediment has undergone greater diagenesis and cementation) the ratio of the dynamic to Wood's bulk modulus increases (Figure 5) and the shear modulus ratio decreases (Figure 6). These results indicate that at relatively high porosities (and low velocities) the Wood's approximation of the bulk modulus, and the estimation of the shear modulus based upon it, are good representations of actual values. Figures 5 and 6 also illustrate the manner in which the Index, calculated from velocity and porosity only, may become a useful tool in obtaining better estimations of shear wave velocities in consolidating sediments.

RESULTS AND DISCUSSION

The inversions for Unit 2, above 340 mbsf, were dissatisfactory. The inversions for this set of data typically converged to minima between .8 and 1.0 km/sec although

the Wood's predictions specified a maximum shear wave velocity more on the order of .6 to .7 km/sec. Occasionally, much worse convergence properties were observed in the Unit 2 data. For example, convergence to unrealistic velocity values leading to Poisson's ratios of less than .25. Finally, there was no indication of even local minima near the predicted shear wave velocities from Wood's equation. Part of this problem can be attributed to the extremely low shear wave velocities in the upper part of Unit 2. Our inversion depends largely on the physical fact that the refracted P wave energy is constantly being converted into shear wave energy at the borehole boundary in order to satisfy the boundary equation, and that this shear wave energy is leaking or radiating away from the borehole and thus lost to the receivers situated in the middle of the borehole. At high Poisson's ratio and low shear wave velocities, the amount of shear wave energy radiating away is largely reduced, going to zero in the limit of a liquid-liquid waveguide. Thus at these velocities the inversion is insensitive to formation shear wave velocities.

From about 340 mbsf of Unit 2 through Unit 3 the convergence properties were radically different. The inversions converged to global minima within 3 or 4 iterations and errors were typically 2 orders of magnitude less than in the case of the Unit 2 inversions. Only in rare cases was there no convergence. Furthermore, the trend in the V_s calculated from the inversion is consistent with that for V_p, porosity, and lithology obtained from conventional logs. Q estimates were also quite reasonable for Unit 3 as shown in Figure 7. Two or three initial velocities were attempted for each inversion as a check on the bounds of the inversion. The Wood's predictions were derived independently from the inversions yet provide an accurate and consistent upper bound on the inversion results.

One thing that became quite evident when processing this large data set is the changing character of the spectra as one proceed deeper downhole. Although it's difficult to show this change with one figure we'll attempt to do so here (Figure 8). The first spectra from Unit 2 shows three distinct peaks at about 8.5, 10.5, and 14 kHz. The bottom pair of spectra shows a coalescence of the latter two peaks although the first peak remains in the same location with respect to the top figure. This implies that there are three P-wave leaky modes present in Unit 2 and only two in Unit 3. The larger the number of leaky modes, the longer the ringing of the P wave train. It is evident from the data that not all the waveform has been captured in some cases, especially with the far receiver. This will significantly affect the result. The extra P leaky mode also makes the forward problem less accurate, since we are approximating the effects of the tool by reducing the borehole diameter. It is known (Cheng and Toksöz, 1981) that the higher modes are less well represented than the first mode in this approximation. This change in spectra has another impact on the convergence properties of the inversion. The deeper results, because of their less jagged nature, would have a smoother spectral ratio and less sensitivity to noise.

CONCLUSIONS

Marine sediments because of their high porosity on one hand and their non-zero shear modulus on the other are not properly modelled by either Wood's equation or the Wyllie time average equation. However, at high porosities, the Wood's equation derived estimate of bulk modulus is fairly accurate. Through differencing the measured P-wave velocity and the Wood's predicted bulk modulus, a reasonable estimate of the maximum value of the shear modulus is obtained. The concept of Acoustic Index used in this paper (Wilkens et al., 1989) bridges the gap in velocity-porosity relationships between high porosity oozes and partially cemented marine sediments.

Using these Wood's equation predictions for the maximum value of the shear modulus, a good agreement was seen with the inversion results for Unit 3. However, the results were disappointing for the lower part of Unit 2. We believe this is due to limitations in the forward model, including the inaccuracy in describing the borehole environment and numerical errors, as well as the limitations presented by noisy data and data not recorded to the end of the wavetrain.

ACKNOWLEDGEMENTS

We would like to thank Mike Simpson and Bob Cunningham, systems operators of the Hawaii Institute of Geophysics, for translating binary data files from VAX to IEEE format in record time, helping to make Jeff's stay rewarding. This work was supported by the Full Waveform Acoustic Logging Consortium at MIT and by National Science Foundation grants No. OCE84-08761, OCE87-10226, and OCE87-20032. Parts of the computing were performed at the Pittsburgh Supercomputing Center.

REFERENCES

Cheng, C.H., Full waveform inversion of P waves for V_s and Q_p, *Full Waveform Acoust. Logging Consort. Ann. Rept.*, 323–338, 1987.

Cheng, C.H., and Toksöz, M.N., Elastic wave propagation in a fluid-filled borehole and synthetic acoustic logs, *Geophysics, 46,* 1042–1053, 1981.

Dandekar, D.P., Pressure dependence of the elastic constants of calcite, *Phys. Rev., 172,* 873–877, 1968.

Hamilton, E.L., Elastic properties of marine sediments, *J. Geophys. Res, 76,* 579–603, 1971.

Hamilton, E.L., Variations of density and porosity with depth in deep-sea sediments, *J. Sed. Pet., 46,* 280–300, 1976.

Hamilton, E.L., and Bachman, R., Sound velocity and related properties of marine sediments, *J. Acoust. Soc. Amer., 72,* 1891–1904, 1982.

Kurkjian, A.L., Numerical computation of individual far–field arrivals excited by an acoustic source in a borehole, *Geophysics, 50,* 852–866, 1985.

Meredith, J.A., Cheng, C.H., and Wilkens, R.H., Determining shear wave velocities in soft marine sediments: *Full Waveform Acoust. Logging Consort. Ann. Rept.,* 339–364, 1987.

Ogushwitz, P.R., Applicability of Biot theory, III. Wave speeds versus depth in marine sediments, *J. Acoust. Soc. Amer., 77,* 441–452, 1985.

Tsang, L., and Rader, D., 1979, Numerical evaluation of the transient acoustic waveform due to a point source in a fluid-filled borehole, *Geophysics, 44,* 1706–1720, 1979.

Wilkens, R.H., Schreiber, B.C, Caruso, L., and Simmons, G., The effects of diagenesis on the microstructure of Eocene sediments bordering the Baltimore Canyon Trough, *Init. Repts. DSDP, 95,* Washington (U.S. Govt. Printing Office), 527–548, 1986.

Wilkens, R., Caruso, L., Simmons, G., The ratio Vp/Vs as a discriminant of composition for siliceous limestones, *Geophysics, 49,* 1850–1860, 1986.

Wilkens, R.H., McClellan, P., Moran, K., Schoonmaker, J.S., Taylor, E., and Verduzco, E., Diagenesis and dewatering of clay-rich sediments, Barbados accretionary prism, *Proc. ODP, Init. Repts. (Pt. B), 110B,* in press, 1989.

Wood, A.B., *A Textbook of Sound,* G. Bell and Sons. Ltd., 1941.

Wyllie, M.R.J., Gardner, A.R., and Gardner, L.W., Elastic wave velocities in heterogeneous and porous media, *Geophysics, 21,* 41–70, 1956.

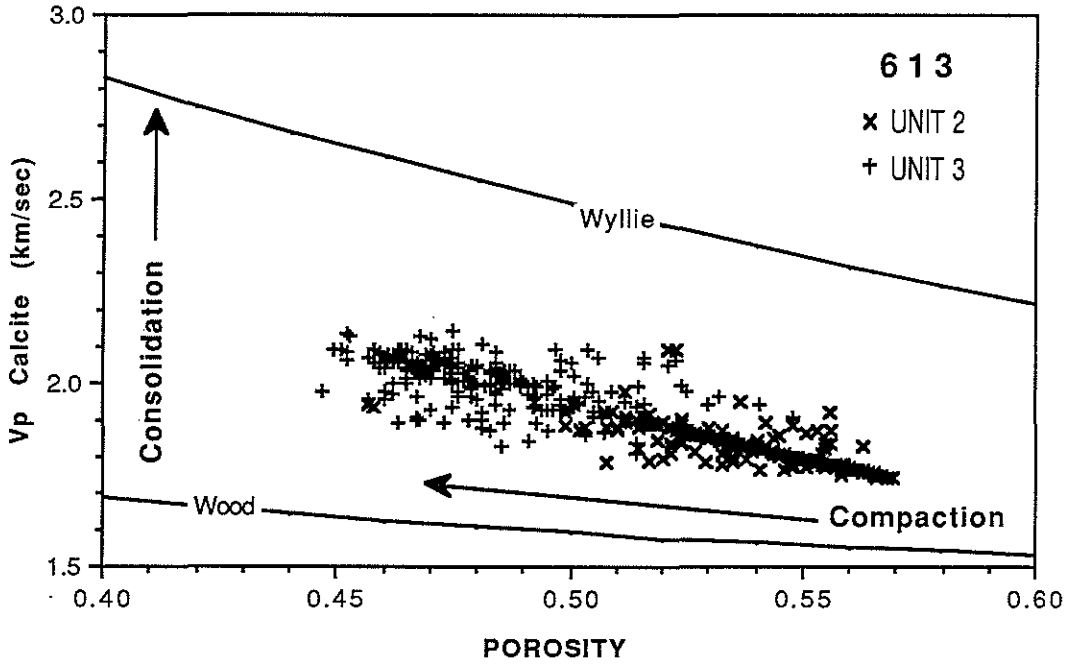

Figure 1: Compressional wave velocity plotted against porosity from Site 613. Also included on the plot are two theoretical velocity-porosity relationships: Wyllie's time average equation (Wyllie et al., 1956) and Wood's equation (Wood, 1941). See text for formulae and discussion.

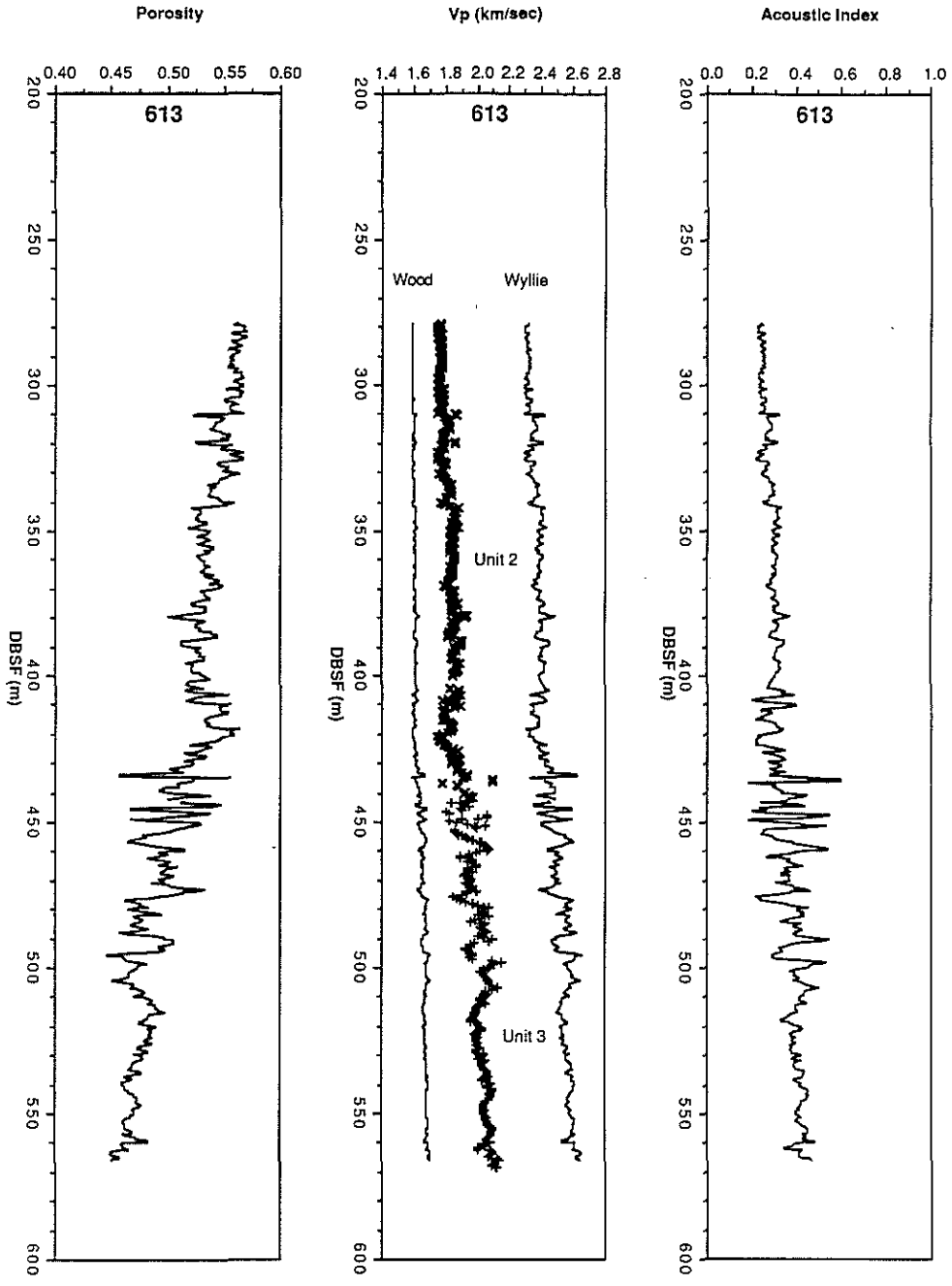

Figure 2: Porosity, compressional wave velocity, and Acoustic Index plotted against depth at Site 613. The Wood and Wyllie compressional wave velocities for calcium carbonate computed from the porosity log are shown flanking the velocity data. The Index reflects the relative position of a data point between the theoretical lines.

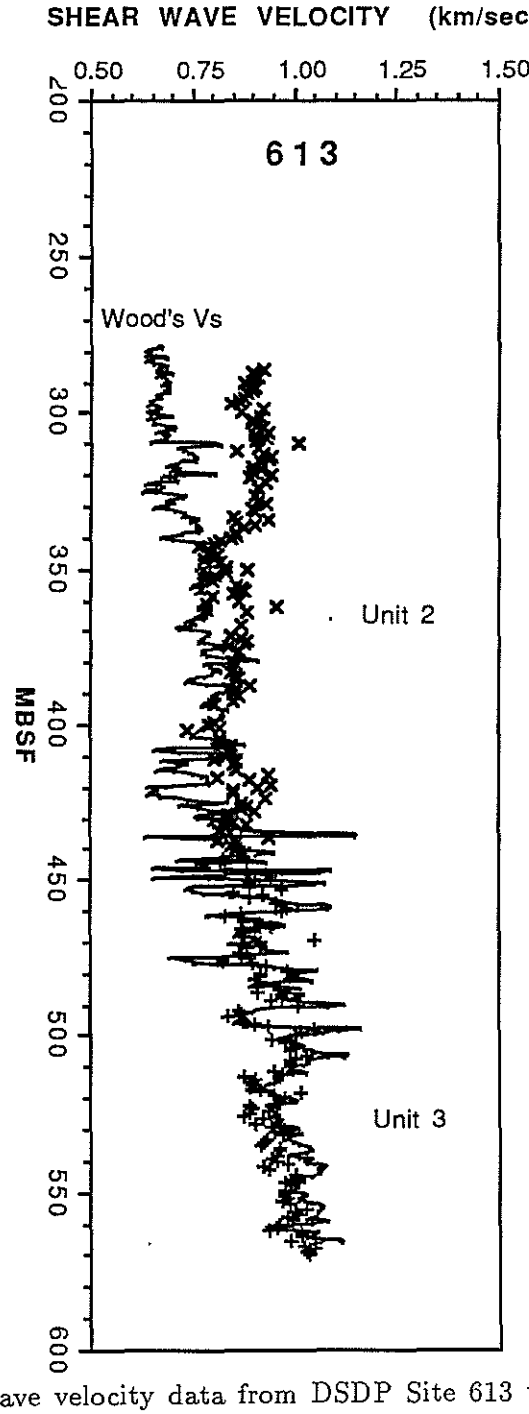

Figure 3: Shear wave velocity data from DSDP Site 613 well logs. Unit 2 is a soft chalk and Unit 3 contains firm chalks and porcellanites. Each symbol represents the result of the inversion of a single waveform. Wood's V_s is an estimate of the shear wave velocity based on well log porosity and compressional wave velocity data (see text).

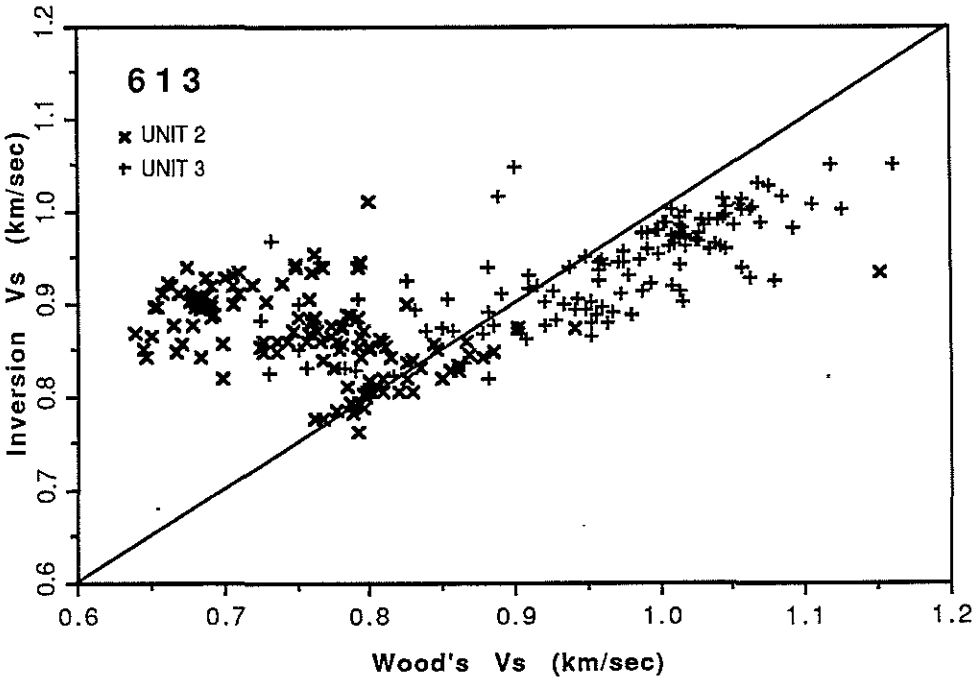

Figure 4: A comparison of well log (inversion) shear wave velocity and predicted shear wave velocity based on Wood's equation (Wood, 1941). The anomalously fast inversion results are from the upper 150 m of Unit 2, an interval where the inversion process breaks down. The line represents Wood's V_s = Well Log V_s.

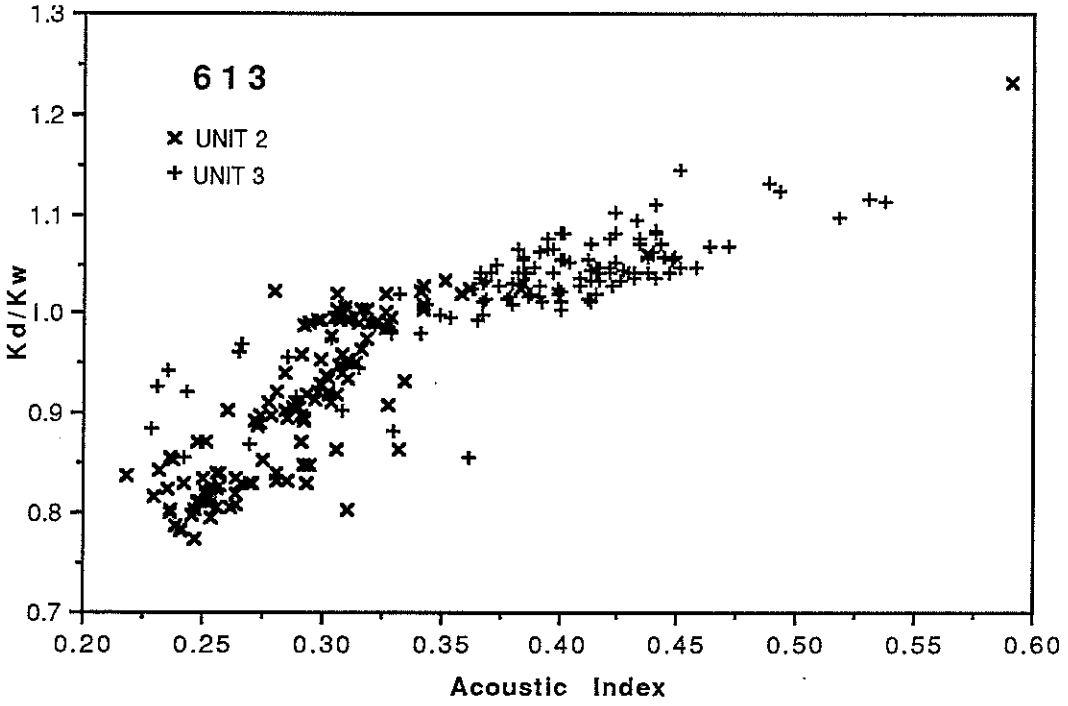

Figure 5: The Acoustic Index at Site 613 plotted versus the ratio of the dynamic bulk modulus calculated from logging and inversion data (Kd) and the Wood's bulk modulus calculated using porosity logs and assuming calcite as the grain material (Kw). The Wood's bulk modulus represents a minimum and the ratio should be equal to 1.0 or greater.

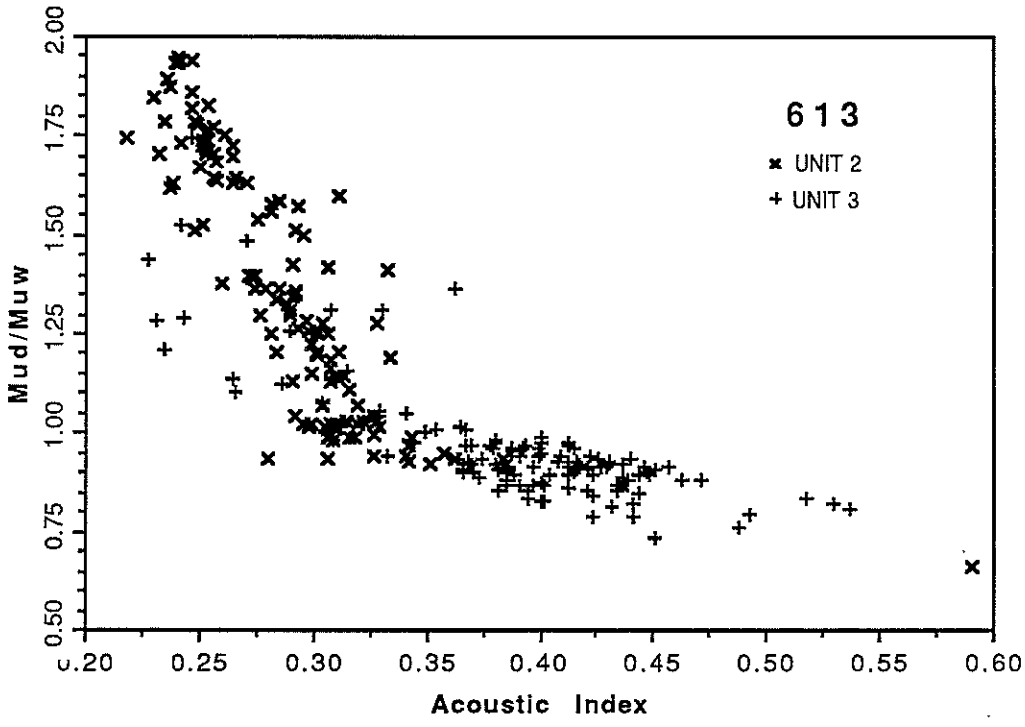

Figure 6: The Acoustic Index at Site 613 plotted versus the ratio of the dynamic shear modulus calculated from logging and inversion data (Mud) and the Wood's shear modulus calculated using porosity logs and assuming calcite as the grain material (Muw). The Wood's shear modulus represents a maximum and the ratio should be equal to or less than 1.0.

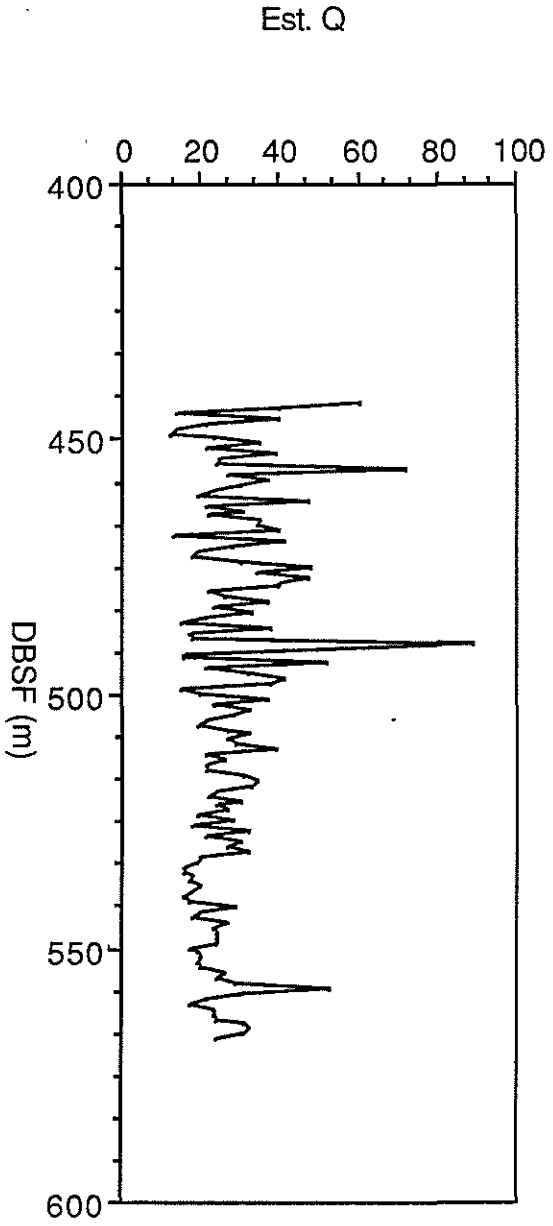

Figure 7: Plot of Q values from Unit 3. Good and reasonably stable estimate of Q.

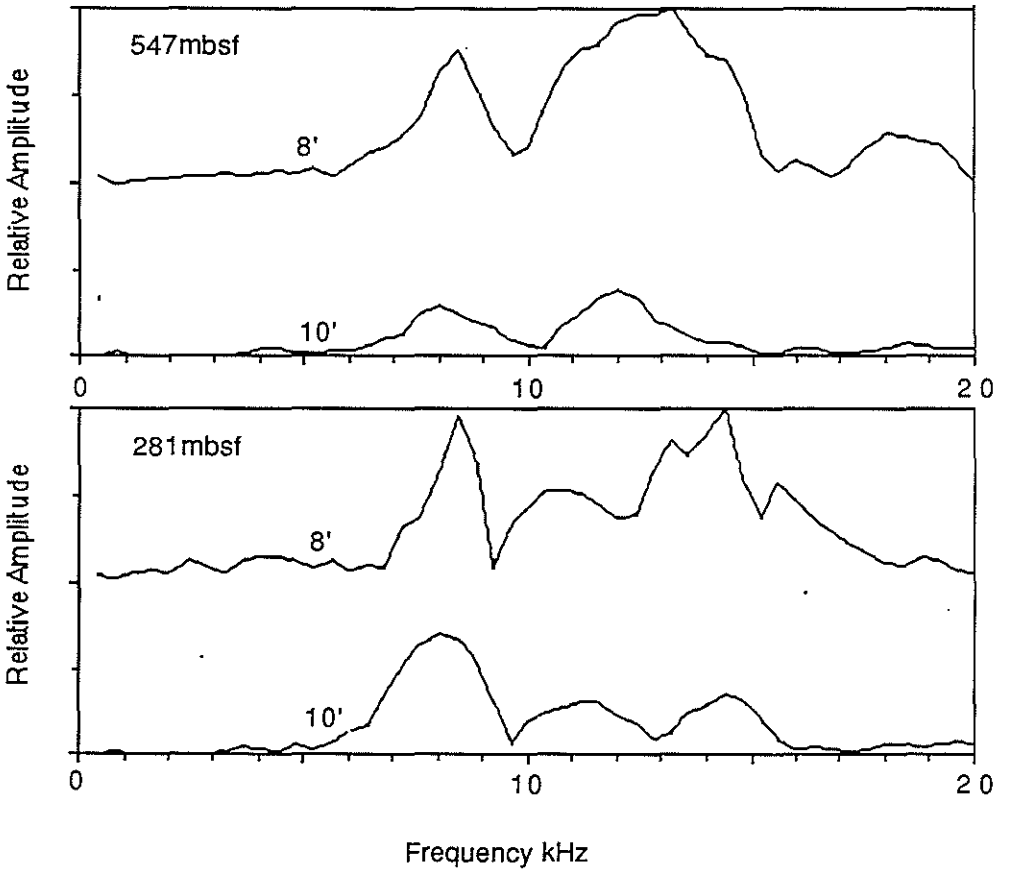

Figure 8: Frequency spectra for the 8' and 10' source receiver separation time series for two different depths. On top are the spectra from the waveforms at 282 meters below sea floor depth (8575.0 ft total depth) from Unit 2. On the bottom are the spectra from the waveform at 548 mbsf (9450.0 ft total depth) from Unit 3. The changes in character and the peakedness are very evident.